Numerical Simulation and Optimization of a Locally Built Midibus Structure in Quasi-static and Rollover Condition

Hailemichael Solomon Addisu[1](✉), Ermias Gebrekidan Koricho[2], and Adino Amare Kassie[1]

[1] School of Mechanical and Industrial Engineering, Institute of Technology, Dire Dawa University, Dire Dawa, Ethiopia
hailasolomon15@gmail.com

[2] Department of Mechanical Engineering, Addis Ababa Science and Technology University, Addis Ababa, Ethiopia

Abstract. Rollover crashworthiness concerns the ability of a vehicle's structural system and components to absorb energies with complete protection of occupants in dynamic (rollover) crash scenarios. First, this study aims to analyze a locally built midibus structure in rollover crashes using numerical investigation (LS-DYNA) as stated by United Nations Regulation 66 (UNECE R66). Also, this study considered the quasi-static simulation to determine the energy absorbing and load-deformation behavior of the midibus frame sections. Then, the two alternatives in design optimization were presented via reinforcement design and numerical optimization (Successive Response Surface Method in LS-OPT) to improve the strength and weight of the midibus structure. As a rollover simulation result, the maximum deformation of the baseline structure occurred at pillar A and three bays. As a result, the baseline midibus structure failed the standard requirement and has unacceptable strength in both quasi-static and rollover simulation. Moreover, related to the baseline model, the structure's weight of the reinforced Model was effectively reduced by 5.2%. However, an optimized model (using the Successive Response Surface Method) has reduced the weight of the reinforced model by 5.6%. Lastly, the Energy Absorption and Specific Energy Absorption of the baseline and the two alternative models were evaluated and compared.

Keywords: Crashworthiness · Deformation · FE methods · Midibus · Reinforcement · Rollover

1 Introduction

Locally built buses (midibuses) and public transport vehicles are frequently used in Ethiopia. Moreover, most buses are locally manufactured in Ethiopia from ISUZU N-Series truck chassis with accessible materials. However, these locally built midibuses are not analyzed and tested using numerical or experimental approaches. Also, for approval,

© ICST Institute for Computer Sciences, Social Informatics and Telecommunications Engineering 2023
Published by Springer Nature Switzerland AG 2023. All Rights Reserved
B. H. Woldegiorgis et al. (Eds.): ICAST 2022, LNICST 455, pp. 95–126, 2023.
https://doi.org/10.1007/978-3-031-28725-1_7

most midibuses are expected to conform to the set parameters, usually spatial (length, width, and height), seating, and weight measurement. However, this approval technique leads to low strength and overheavy bus structure [1]. Moreover, rollover crashes frequently happen due to the reasons of rolling down into a cliff, collision with vehicles and rotating sideways by obstacles (ditch, kerb, or objects) [2–4]. Most rollover crashes happen on the road of curved (tangent) sections in Ethiopia due to the pedestrian's priority and fast-moving (high speed) crashes [5]. Additionally, bus rollover accidents occur under the circumstance of dropping down into a cliff in this country. Consequently, These accidents led to 50% of fatalities and 50% of passengers' injuries in 2004 [6]. Mainly, the bus rollover accidents obtained serious structural deformation and severe injuries & fatalities to the passengers [2, 3]. The public transport vehicles (buses) involved high numbers of fatalities and injuries during crashes. In Ethiopia, fatalities by bus crash involved nearly 35.42% (1,324 road traffic deaths) in 2018. (UN ECE 2020) reported that in Ethiopia, the crash tendency increased on average by 9% from 2010–2018 [7]. Specifically, rollover crashes consist of 17.34% fatalities & 17.17% of injuries within six years (2005–2011) [5].

Crashworthiness is the ability to absorb vehicle crashes and protect the occupants in survival space [8, 9]. Structural crashworthiness is concerned with designing a vehicle's structural system and components, which requires absorbing the dynamic energies and loads and energies in dynamic case (collision (impact) occasion) [10, 11]. Therefore, after the design of the bus, the numerical simulation by FE Method is a better approach to visualize the strength and decrease the development time of the bus before manufacturing and testing. In a quasi-static analysis, (Micu et al., 2014; Nurhadi & Zain, 2010) [12, 13] presents a study of quasi-static loading test on bus body sections by regulation of UNECE R66 via both FEM simulation (ANSYS) and experimental test. Likewise, (Nor & Baharin, 2014) [14] studied a quasi-static simulation test by ANSYS Explicit Dynamic Analysis using the standard of UN ECE R66. According to (Mahajan et al., 2003; Na et al., 2014) [15, 16], the bus structure resistance of rollover by experimental setup for the rollover test of bus section and numerical model with FEM (LS-DYNA solver). Moreover, (Bai et al., 2019; Phadatare, 2017; Rogov Petr Sergeevich & Orlov Lev Nikolaevich, 2015; Thosare & Patil, 2017; Zhou et al., 2019) [2, 17–20] studied the rollover of a bus frame (structure) analyzes by the experimental method and detailed FEM method. Also, (Wang, Pan, Zhang, & Cui, 2015) [32] discussed and analyzed the system's energy dissipation and the effects of energy-absorbing of the main structure in the rollover crash process using experiment tests and FE model. Again, (Yang & Deng, 2015) [21] analyzed and studied the structural optimization and lightweight of the bus body skeleton using the numerical Model by Hyperworks.

M. K. Mohd Nor & M. Z. Dol Baharin, 2014) [14] studied the numerical simulation (ANSYS) of a heavy vehicle bus structure according to FMVSS 220 & ECE R66 for quasi-static and rollover analysis. Lastly, (Karliński et al., 2014) [4] focused on the strength of the Volkswagen LT vans bus structure according to ECE R66 using a numerical model & simulation using FEM. (Korta & Uhl, 2013) [22] analyzed and studied multi-material optimization of bus structure using Genetic Algorithm (GA) optimization and numerical simulation for different materials. Similarly, (Reyes-ruiz et al.,

2013) [23] optimized and analyzed the passenger bus frame by using the design concept, numerical analysis, and simulation for different materials with FE Method on the parameters of strength (torsion, bending), dynamics (vibration response) constants and the thickness of bus frame structure. Then again, (Hu et al., 2012; Li et al., 2012a; Yusof & Afripin, 2013) [24–26] studied that bus superstructures undergo rollover events through experimental tests and numerical simulation with FEM. Lastly, (Su et al., 2011; Yusof et al., 2012) [3, 27] discovered the bus frame and validated it through a single box model experiment and FE analysis for the masses effects and bus structure strength.

Consequently, (Bojanowski & Kulak, 2011; Tech & Iturrioz, 2009) [28, 29] studied the bus structure using numerical simulation with FEM by LS-DYNA, Multi-Objective (MO) Optimization, and optimization by super-beam elements by plastic hinge lateral-base union of two samples. On the other hand, (Matolcsy 1997) [30] focuses on severe conditions and parameters in rollover accidents of bus structures through statistical and qualitative data analysis using standards and general testing methods. (R. P. Sergeevich & O. L. Nikolaevich, 2015) [20] focused on verifying and analyzing the bus body structure components in the rollover test by experimental and numerical crashworthiness investigations of the bus structure for each element. According to (Friedman et al., 2006) [31], the composite roof structures in transit buses are implemented and analyzed. (Lan et al., 2004; Cho Chung Liang & Le, 2009; Lin & Nian, 2006) [32–34] studied the design and analysis of the bus frame structure during a rollover by numerical simulation of bus structure sections and optimized through LS-OPT (successive_respond_surface_method (SRSM)). (Rahman, 2011) [35] The numerical modeling and analysis of the middle section of the bus structure are only designed and analyzed. According to (Park et al., 2006) [36], the beam's analytical and numerical Model and non-linear spring elements of the bus structure in a rollover are discussed. (Tech et al., 2007) [8] studied experimental and theoretical predictions of the collapse of basic bus structure with FEM (LS-DYNA) for plastic hinges by a super-beam element of the bus section in a rollover. (C. C. Liang & Nam, 2010) [37] studied the bus rollover protection using the numerical simulation using FEM (ANSYS) according to ECE R66 & FMVSS 220. (Subic & He, 1997) [38] discussed the experimental and analytical modal analysis of the bus roll-cage structure by an Alternative Research Approach. And also (Bojanowski et al., 2011; Valladares et al., 2010) [39, 40] studied the experimental setup and numerical Model of a paratransit bus for roof crush and rollover.

Accordingly, this study mainly focuses on the rollover crashworthiness analysis and optimization of the locally built midibus structure with the FE Approach according to UNECE R66 Standard. Foremost, the existing midibus structure is carefully studied using FE Method (LS-DYNA) according to the testing standard of UNECE R66. This approach visualizes which structure components lead to low strength and overweight. And then, two techniques of structural optimization were developed, structural modification (reinforcement) and numerical optimization (SRSM) in LS-OPT. Lastly, the comparison of the three models (baseline, reinforced (Model – I), and optimized (Model – II) model) was measured according to the structural strength and weight.

2 Methodology

In Ethiopia, the size of the midibuses depends on the chassis model types and specifications used by local manufacturers. Nevertheless, local manufacturers commonly used ISUZU NPR 71K chassis to manufacture a midibus in Addis Ababa, Ethiopia [1]. Hence, this study focuses on the locally built midibus (using ISUZU NPR 71K chassis model), which has a twenty-nine (28 + 1) passenger capacity. And also, the mass of the unladen kerb (M_k) and Gross Vehicle Weight (GVW) are 4500 kg and 7350 kg, respectively. The existing (baseline) model of a locally built midibus structure has six parts: front, roof, rear, floor, left, and right frame, as shown in Fig. 1. Therefore, the FE Model development consists of quasi-static and rollover crash analyses of the midibus structure. LS-DYNA is the best and most efficient for explicit dynamic analysis because of using a return mapping algorithm and the central difference method to avoid expensive numerical iteration and matrix inversion [41]. Accordingly, the rollover crash FE analysis with the quasi-static FE analysis is developed using the explicit code of LS-DYNA R11.0 as stated by the standard of UNECE R66.

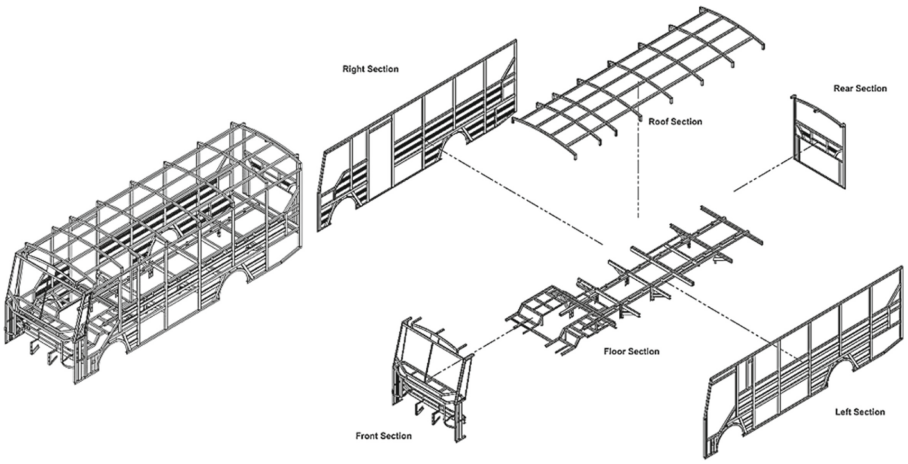

Fig. 1. Main parts of the baseline midibus structure

The material used for all parts (sections) of the bus frame is conventional structural steel. Moreover, the material properties of conventional structural (CS) steel, such as *density (kg/mm^3), Yield Strength (MPa), Ultimate Tensile Strength (MPa), Elongation (%), and Young's Modulus (MPa)* are *7850, 260, 360, 30, 210, respectively*. Consequently, the material input data of the FE Simulation needs the effective stress versus the effective plastic strain curve, as shown in Fig. 2.

The input data of the material in numerical simulation (LS-DYNA) needs the effective stress versus the effective plastic strain curve. The true stress (σ_t) and the true plastic strain (ε_t) determined by:

$$\sigma_t = \sigma_{eng}(1 + \varepsilon_{eng}) \tag{1}$$

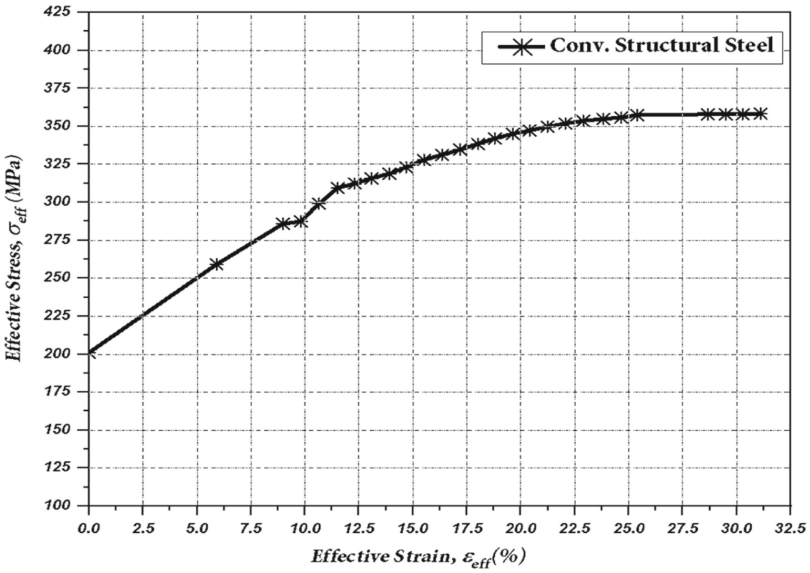

Fig. 2. Effective stress vs plastic strain curve for conventional structural steel

$$\varepsilon_t = \ln[1 + \varepsilon_{eng}] \tag{2}$$

where: σ_{eng} - the engineering stress and ε_{eng} - the engineering strain.

2.1 Quasi-static and Rollover Simulation Using ECE R66

Procedures for the Quasi-static Analysis

The quasi-static simulation uses to check whether the bus sections and their bays withstand the rollover crash or not [42, 43]. Hence, the body sections and their bays evaluate whether they failed or passed the quasi-static loading test. Once studying structure roof-crush and buckling behavior, the LS-DYNA explicit time integration is the best to bring reliable results [44]. Thus, the quasi-static simulation procedures have been done according to UNECE R66 using explicit code in LS-DYNA Software to study and analyze the bus structure energy absorbing and load-deformation behavior. This paper develops the bus superstructure model as a shell element for fast and high computational simulation. The selected Belytschko-Lin-Tsay shell element is defaulted to calculate the shell element formulation in LS-DYNA R11.0. Moreover, this shell element has high computational efficiency compared to others [42, 45]. Furthermore, the residual space and rigid plate (impactor) model are developed for the quasi-static simulation, as shown in Fig. 3.

The FE model for quasi-static simulation is developed as a shell element (quadrilateral and triangular), as shown in Fig. 3. Also, due to the variation of frame size, the maximum and minimum element sizes of the bus body frame are 10 mm & 2.5 mm. Thus, the total quasi-static FE model consisted of 885,722 shell elements with 905,923

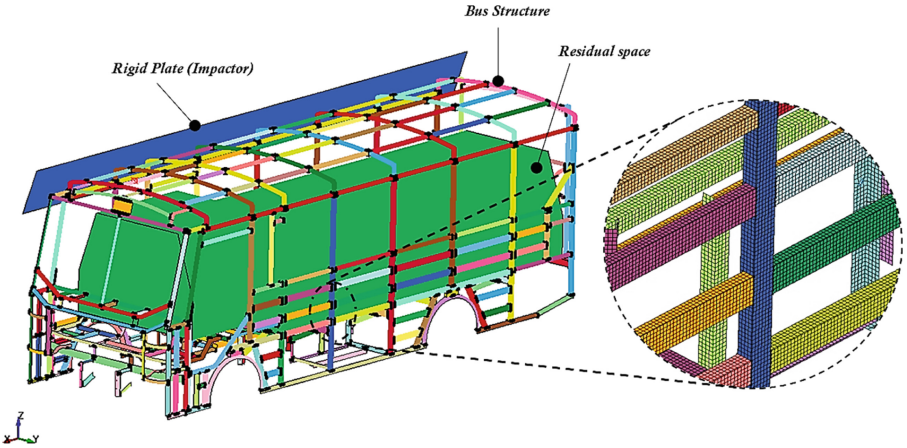

Fig. 3. FE Model for quasi-static simulation

nodes with an average element size of 15 mm (see Table 1). Hence, the weld formulation between all frame parts is modeled as spot welds (rigid nodes) through the 'CONSTRAINED_SPOTWELD' card without defining the failure force [26, 42, 46–48]. Experimental material properties of structural steel were executed into the FE models formulation. The PIECEWISE_LINEAR_PLASTICITY (MAT_24) material definition was implemented [42]. A rigid plate (the impactor) is developed by the material model of Rigid (MAT_20). A null (MAT_09) material is used to represent occupant space.

Table 1. Statistics of the existing (baseline) FE Model for the quasi-static analysis

Description	Bus structure	Residual Space & Impactor	Entire Model
Material type	Pieces-wise Linear Plasticity (MAT_24)	Rigid (MAT_20) & Null (MAT_09)	-
Min. element size (mm)	2.5	-	2.5
Max. element size (mm)	10	15	15
Number of parts	355	2	357
Number of nodes	572,578	333,345	905,923
Number of elements	553,040	332,682	885,722

Loading and Boundary Conditions. During the simulation, the rigid rectangular plate (impactor) touches the roof frames at an angle between the vehicle's longitudinal vertical center plane (VLCP) and the load direction [43]. A quasi-static load is distributed on the cant rail section with a rectangular plate (impactor). Thus, the quasi-static loading rate is applied quasi-equally for the 500 mm displacement with a short incremental time

of 2.25 s. However, the computational time of the simulation takes 1.75 s to reach the passenger compartment. The external load card 'LOAD_BODY_Z' is applied as the gravity of the bus structure.

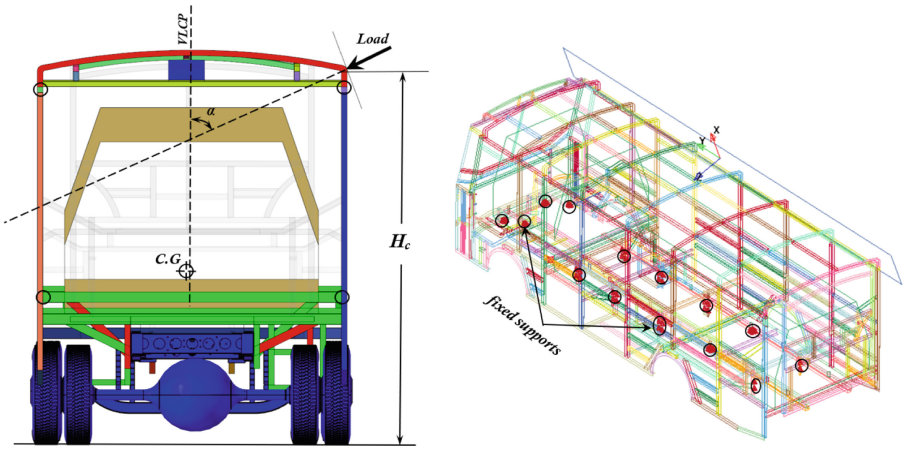

Fig. 4. Loading direction (left) and fixed supports (right) in the quasi-static simulation.

The fixed supports are causing no effect on the structure's deformation. These supports are applied to the underfloor structure section (see Fig. 4 (right)). The angle between the load direction & the vehicle's longitudinal vertical center plane (VLCP), (α) is determined by

$$\alpha = \frac{\pi}{2} - \sin^{-1}\left(\frac{800}{H_c}\right) \tag{3}$$

where: H_c- height of the vehicle's cant rail (in mm) from the horizontal plane (see Fig. 4 (left)).

The penalty-based contacts are contacts algorithms used in crash simulation [47]. The contact algorithm of 'AUTOMATIC_SINGLE_SURFACE' is appropriate for self-contacting cases. This contact type was used to state the contact between all bus section components. The contact 'AUTOMATIC_SURFACE_TO_SURFACE' is defined as the contact relationship between the bus section and a rigid plate (impactor). The static and dynamic friction coefficient for steel-to-steel contact is a value of 0.15 and default, respectively [49].

Evaluation Criteria for Quasi-static Simulation Results. According to the UNECE R66 standard, the minimum energy absorbed by the structure (body sections) (Emin) is equals to the sum of the energy of the ith bay and calculated by:

$$E_{min} = \sum_{i}^{s} E_i = E_T \frac{\sum_{i}^{s} m_i}{M} \tag{4}$$

Then, the total absorbed Energy (E_T) by the vehicle is calculated by:

$$E_T = 0.75\,Mg\ \Delta h \tag{5}$$

where: $M(M_k)$ – the unladen kerb mass of the vehicle, g – the gravitational constant (9.81 m^2/s), Δh – the vertical distance of the vehicle center of gravity in the rollover test, - the energy absorbed by the "i^{th}" bay, and m_i – the mass of the "i^{th}" bay.

By substituting Eq. (5) into Eq. (4), the minimum energy absorbed by the structure (E_{min}) is determined by:

$$E_{min} = 0.75\,g\ \Delta h \sum_{i}^{s} m_i \tag{6}$$

In the quasi-static loading test, the energy absorbed by the structure ($E_{st,a}$) passes if:

$$E_{st,a} \geq E_{min} \tag{7}$$

Otherwise, the structure fails the tests, even if only one of the bays is touched the residual space. Moreover, energy absorption ($E_{st,a}$) and reaction force are indicators of the crashworthiness capability of the structure. The energy absorption ($E_{st,a}$) of the structure can be determined by integrating of the load-displacement curve. Furthermore, it can be formulated by:

$$E_{st,a} = \int_0^l P d\,\delta \tag{8}$$

where: P – applied load (reaction force), l – length of the crushed structure, and δ – displacement.

The specific energy absorption (SEA) is also vital to the design of structural parts that involve the reduction of weight of the structure. Therefore, the Specific Energy Absorption capacity define as the energy absorbed per the mass of the structure [50] and determined by

$$SEA = \frac{E_{st,a}}{m} \tag{9}$$

where: m – mass of the structure.

Procedures for Rollover Analysis.

According to the UNECE R66 standard, the rollover test of a vehicle is used to evaluate the crashworthiness capability and occupant safety during rollover crashes. The rollover crashworthiness via finite element analysis (FEA) is extensively done due to the experimental test's long time and extreme cost [2]. In the bus rollover crash, passenger safety is affected by structure, seats, and seat belt strength [51]. In this study, the bus structure and seat frames are the main components of the bus to study the strength and crashworthiness behavior using LS-DYNA with the explicit time integration code. Moreover, the tare-weight load (Unladen Kerb Mass (M_k)) of the locally built midibus (NPR 71K

Table 2. Components of Unladen Kerb Mass (M_k) of NPR 71K Chassis midibus

Items	Qty	Total mass (kg)
Seat (each 8.5 kg)	29 + 1	255
Self-weight of the structure	–	577
Chassis body with fuel tank, engine, and battery, wheel, axle (NPR 71K)	–	3668
Unladen Kerb Mass (M_k)		4500

Chassis midibus) is 4500 kg (4.5 tons). Table 2. Illustrates the quantities and masses of components in the case of tare weight loading.

In this study, the bus skin, glasses, and other sensitive parts of the vehicle are not modelled due to the difficulty of modelling and simulation. However, the structure and seat are developed by direct measurement from local manufacturers (bodybuilders). First, the chassis components are modeled using the ISUZU N-series body builder manual and guide [52–54]. However, the structure and seat are developed by measuring and observing the bus construction from the available local manufacturers (bodybuilders). Then, the bus structure, chassis, seat frame, tilt platform, and other assembled components were imported to the LS-Prepost as an Initial Graphics Exchange Specification (IGES) file format to develop a finite element mesh.

As shown in Fig. 5, the main parts of the bus structure, such as the cant-rail, window rail, waist rail, A & B pillar, vertical pillars, and skirt rail, are mentioned. Moreover, the structures' eight bays (B1–B8) are also arranged.

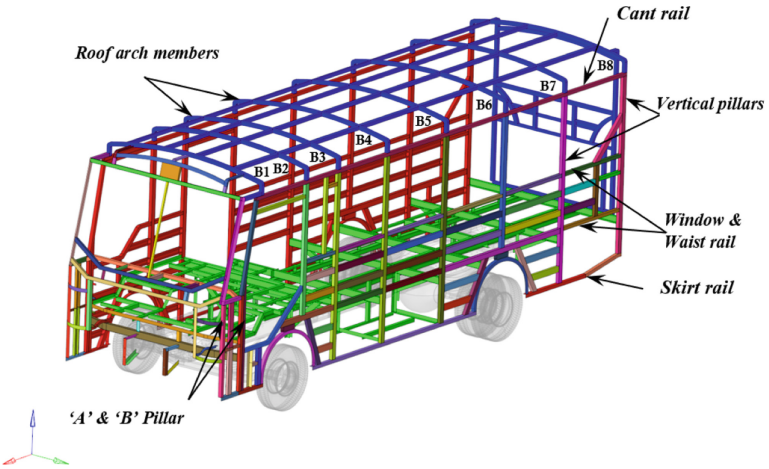

Fig. 5. Components of existing bus body structure

To decrease the computational time of the simulation, the entire rollover model is developed as a Belytschko-Lin-Tsay shell element. However, the thickness of the shell

element is defined by its section properties and values. Hence, the weld connection between all structural parts with seats frame and rail is modeled as spot welds (rigid nodes) using a card 'CONSTRAINED_SPOTWELD' without defining the failure forces and coefficients [26, 42, 46–48]. The keyword 'CONSTRAINED_RIGID_BODIES' defines the assembly between the rigid parts of the chassis by assigning one of them as a master part and merging the others [55].

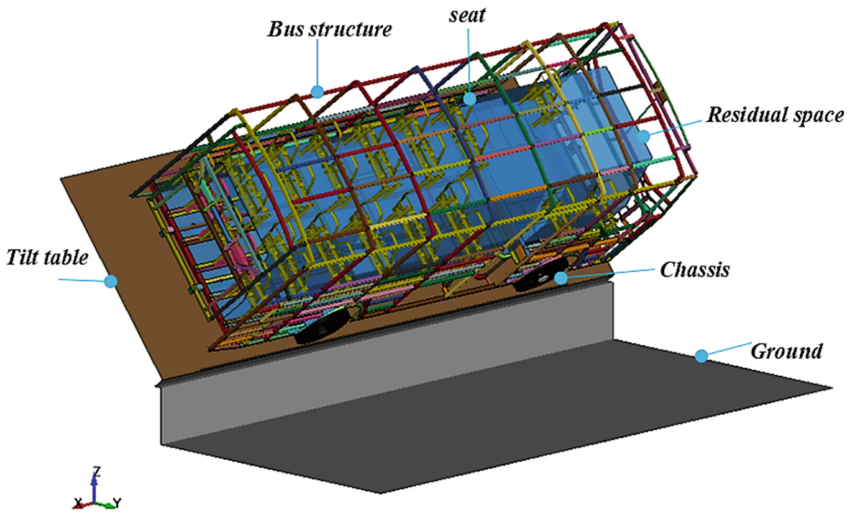

Fig. 6. FE Model for rollover simulation

The bus structure, chassis, seat frame, tilt table, ground, residual space, and element mass of other components are considered for the tare-weight vehicle rollover simulation without bus skin and other deformable parts, as shown in Fig. 6. Also, in this study, the bus skin, glasses, and other sensitive parts of the vehicle are not considered because of their difficulties in modeling and simulation.

In this section, the bus structure element size is constructed similarly to the quasi-static analysis case. The entire rollover FE Model consisted of 1,771,305 shell elements with 1,790,729 nodes (see Table 3.). The overall existing tare weight FE Model contains 412 parts. Hourglass control type (type 4, 5) defines ranges of coefficient between 0.03 to 0.05 for parts of the structure, which is used to reduce the response of non-physical stiffening [56]. The shell elements of FE models, such as fully integrated (type 16) and Belytschko-Tsay (type 2) elements, are the most accurate and have high computational efficiency in crashworthiness simulation [46]. Thus, this study also conducts Belytschko-Tsay (default type) shell element and hourglass control type 4 with a coefficient of 0.05 for all FE rollover models. The computational time decrease when the entire rollover model is developed as a Belytschko-Lin-Tsay shell element.

Table 4 describes the mesh quality of the rollover FE model. The numbers of quadrilateral and triangular elements are 1,757,153(99.2%) and 14,149(0.799%), respectively. Hence, the weld connection between all structural parts with seats

Table 3. Statistics of baseline FE model for rollover simulation

Parameters	Bus structure and seat frame	Tilt table, residual space & ground	Chassis body	Entire model
Min. element size (mm)	2.5	–	–	2.5
Max. element size (mm)	10	15	30	30
Number of Parts	391	3	18	412
Number of Nodes	904,442	818,935	80,076	1,790,729
Number of Elements	885,012	805,934	88,718	1,771,305

frame and rail is modeled as spot welds (rigid nodes) using a card 'CONSTRAINED_SPOTWELD' without defining the failure force [26, 42, 46–48]. The keyword 'CONSTRAINED_RIGID_BODIES' defines the assembly between the chassis' rigid parts by assigning them as a master part and merging the others [55]. The material properties of the rollover structure are similar, as mentioned in the quasi-static analysis. The material model used for all structural frames and seat rail is executed by using PIECEWISE_LINEAR_PLASTICITY (MAT_24) material definition [4, 34, 42, 49]. In most rollover impacts, the chassis parts are in motion but not directly affected by the crashes [57]. Hence, the chassis, tilt table, and ground are developed by rigid material models (MAT_20). A Null (MAT_09) material is used as a symbolic representation for occupant space [58].

Table 4. Summary of shell element quality report for rollover FE model

Criteria	Allowable (threshold) value
Min side length (mm)	3
Max side length (mm)	30
Aspect ratio	10
Warpage	10
Min quad. angle (deg)	45
Max quad. angle (deg)	135
Min tria. angle (deg)	30
Max tria. angle (deg)	120
Taper	0.7
Skew (deg)	45
Jacobian	0.6
#Quads (%): 1,757,153 (99.2%), #Trias (%): 14,149 (0.799%)	

In the rollover simulation, 'ELEMENT_MASS_NODE_SET' is used to lump the mass of passengers, luggage, battery, and engine [46, 59, 60]. In this study, the mass element of the passengers is assigned to the seat frame node. And also, the mass of luggage, battery, fuel tank, engine, and other miscellaneous parts are equally distributed on the chassis and structural components of the bus. During the rollover simulation, the complete vehicle is initially tilted in an unstable (equilibrium) position and a ditch of 800 mm [43]. The angle of the tilt table shall be greater than 35° and the trial & error simulation is needed to obtain the minimum tilt table angle that is used to trigger the vehicle to tip over [48, 61]. Hence, the minimum angle of the tilt table is 49° in an unstable equilibrium position. The bus's initial angular velocity should not exceed 0.0875 rad/s (5 deg/s) [43]. The external load card 'LOAD_BODY_Z' is applied as the gravity of the bus [58]. Furthermore, A card 'INITIAL_VELOCITY_GENERATION' defines the initial angular velocity of the bus [62].

The contact algorithm 'AUTOMATIC_ SURFACE_TO_SURFACE' defines the contact relationship between the structure & ground. Moreover, the coefficient of friction for steel-to-concrete contact is 0.65 [17, 42, 63, 64]. The contact definition between tilt table & tires (rubber-to-steel) is developed using 'AUTOMATIC_NODE_TO_SURFACE' [36]. In this contact, the value of the coefficient of friction is 0.7 [42]. The self-contact between bus body frames (bus section components) and seats (steel to steel) define using 'AUTOMATIC_SINGLE_TO_SURFACE', with its coefficient of friction is 0.15 [42]. Moreover, The Switch 'DEFORMABLE_TO_RIGID_AUTOMATIC' was highly recommended for flexible switch activation and easy use application. This switch is commonly used for a component to switch deformable as well as rigid automatically by the change of contact surface force or rigid wall force [17, 65, 66] hence, the rollover simulation of a vehicle needs to change from deformable material to rigid material or vice versa using a 'DEFORMABLE_TO_RIGID_AUTOMATIC' switch. The first switch activates all model parts, from deformable to rigid. The second switch activates only the structure and seat with seat rail to deformable material. The two switches are paired and related to each other to switch back and forth using a contact force automatically.

The overall rollover simulation (Elapsed) time took over two days (48 h) by using the Intel CORE (R) i7-7700HQ CPU @ 2.80 GHz processor, depending on the initial and finish contact time. For accurate energy distribution with stable models during simulation, the option of mass-scaling was considered to regulate the time step (DT2MS) [57]. During the tare–weight rollover case, the time step is reduced from 1.00e−5 to 1.00e−6 s between simulation time of 1.62–2.25 s. This rollover procedure is used to minimize computational time [42]. However, the computational time of the simulation takes 2.25 s until the vehicle reaches motionless.

FE Verification of Energy Balance in Rollover simulation. The numerical simulation error assesses by the task of the model verification of the FE model [46]. In the rollover simulation, checking the energy balance is the main factor in assessing the solution's errors. this verification guidelines presents the concept of energy conservation laws [42, 46, 67]. The applied total energy of the structure can be determined as stated by ECE

R66 [43]:

$$E_{Total} = 0.75\,Mg\ \Delta h \text{ or}$$

$$E_{Total} = 0.75\ Mg\left(\sqrt{\left(\frac{W}{2}\right)^2 + H_o^2} - \frac{W}{2H}\sqrt{H^2 - (800)^2} + \frac{(800 * H_o)}{H}\right) \tag{10}$$

where: W – the overall width of the bus, I – the height of the bus, and H_o – the height of the center of gravity.

The LS-DYNA total energy (E_{Total}) is the sum of six components such as current internal energy (E_I), current kinetic energy (E_K), current sliding energy (E_{Sli}), current hourglass energy (E_{HG}), current system damping energy (E_D), and current stonewall/rigid wall energy (E_{RW}) and also must be equal with the sum of initial total energy ($E_{Total,o}$) & work done by external loads (W_{Ext}) [68, 69]:

$$E_{Total} = E_K + E_I + E_{Sli} + E_{RW} + E_{Damp} + E_{HG} = E_{Total,0} + W_{Ext} \tag{11}$$

$$E_{Total,0} = E_{K_0} + E_{I_0} \tag{12}$$

where: E_{I_0} – the initial internal energy & E_{K_0} – the initial kinetic energy

Angular Deformation Index (DI_θ) is a quantitative measure used to evaluate a margin of safety and a deformation extent in rollover simulation [42, 46]. Thus, this index also measures the structure's strength during rollover crashes. Figure 7 shows the angle between wall & floor ("$_3$), angle of waist rails (θ_2), and angle between roof & wall (θ_1) with a measured angular deformation. The Angular Deformation Index (DI_θ) can be determined as [46]:

$$DI_\theta = \frac{l}{400}\tan(\Delta\theta_3) + \frac{(1250 - l)}{400}\tan(\Delta\theta_2) \tag{13}$$

where: $\Delta\theta_3$ – the angle changes between wall & floor, $\Delta\theta_2$ – the angle changes of waist rails and l – the distance from the floor to waist rails.

2.2 Structural Reinforcement and Optimization of the Structure

Optimization is the development of objective functions with constraints to maximizing or minimizing the desired value [70]. In the computer-based optimization process, the simulation requires a high number of iterations, the performance of computers, and large numbers of design parameters [46]. However, reinforcement optimization is a technique to strengthen the vehicle's body [1, 71]. Therefore, this study's primary goal is to specify the two alternative design solutions. However, this process was done by use of practical reinforcement (model – I (RD)) and numerical optimization technique using the Successive Response Surface Method (SRSM) in LS-OPT (Model – II (SRSM)) for dynamic (rollover) conditions.

Structural Reinforcement Design.

Most local bus manufacturer experiences the design of the structure's construction

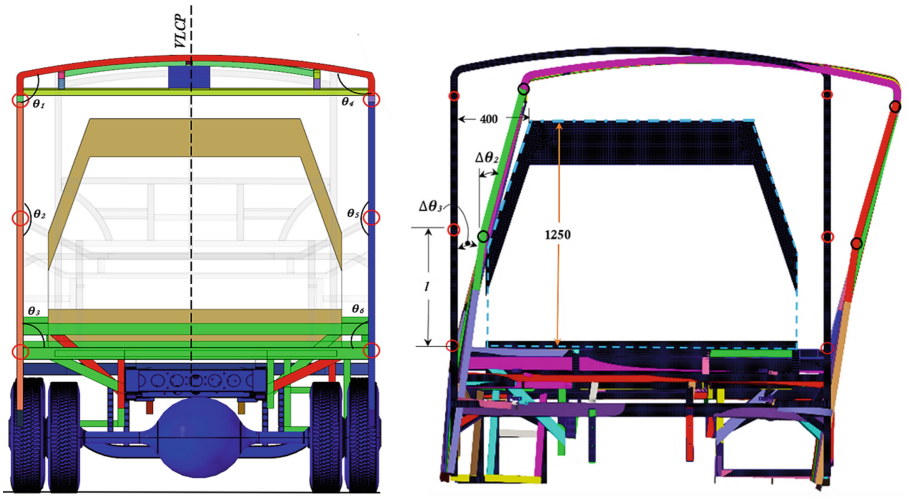

Fig. 7. The concept of deformation angle and angular deformation index [46]

through the try and error methods, this approach outcomes in low structural strength and safety of the passengers during accidents. The existing bus structure needs a structural design analysis and improvement to maximize the strength and minimize the structure's weight. First, the existing bus structure carefully examines using the manufacturer constraint and the dynamic rollover simulation to select the component's layout and cross-sections that might be changed. When these components lead to low strength, the change in in the cross-section and layout of structural components were measured. As shown in Fig. 8, the most local bus bodybuilder used the wall support members as support and cover of the walls. However, Due to high number of wall support, the weight of the bus structure was increased. Even though, these components do not strengthen the bus structure in rollover conditions due to their arrangements and cross-sections.

In this study, the design modification (reinforcement) conducts the addition and replacement of the structural components. First, the layout of the structure and the shape of the cross-section in the structural elements are changed. Next, the supports were added to assemble the section of the structure. As a result, the rectangular (lying orientation) profile has a much higher energy absorption for oblique impact load directions than the square cross-section [72]. The other important consideration for the rollover case is the strength of the floor-wall connection. Hence, the supporting member attaches at the corner of the floor and sidewall section on the front, medium, and rear portions to reduce the structural deformation.

Accordingly, the baseline design defects improve through additional support and change the layout and cross-section of the structure, as shown in Fig. 9. Therefore, the new modified (reinforced) midibus structure has been considered the following structural design modifications:

- Roof arc members to strengthen the roof -parts using rectangular cross-section (RHS)

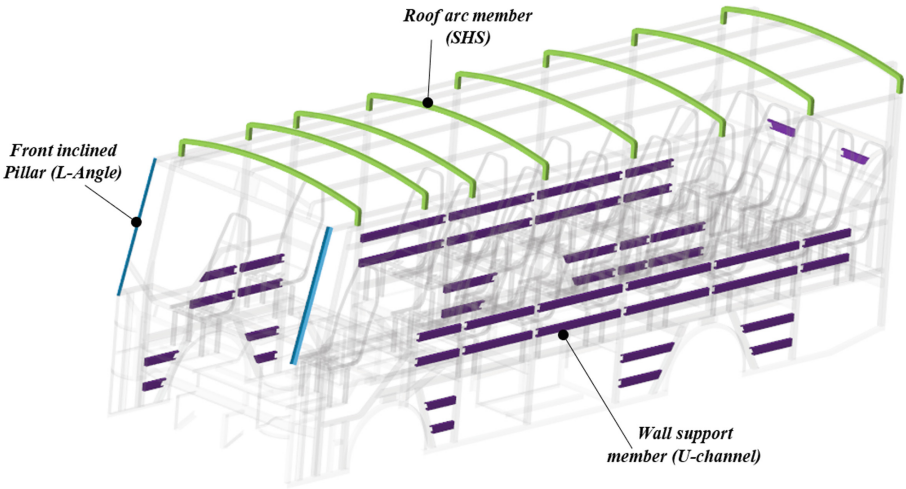

Fig. 8. Selected Configurations to improve the baseline design

- Inclined connecting elements (Supporting members – #1) at the left & right sections of frames
- Supporting members from #2 to #4 developed to build a connection between roof and sides pillars with rear pillars, Support for extended floor section & chassis, and Support for connection side walls and floor during the rollover, respectively
- Inclined front (A) pillar at the front section of the structure (square cross-section (SHS)) to strengthen the front pillar

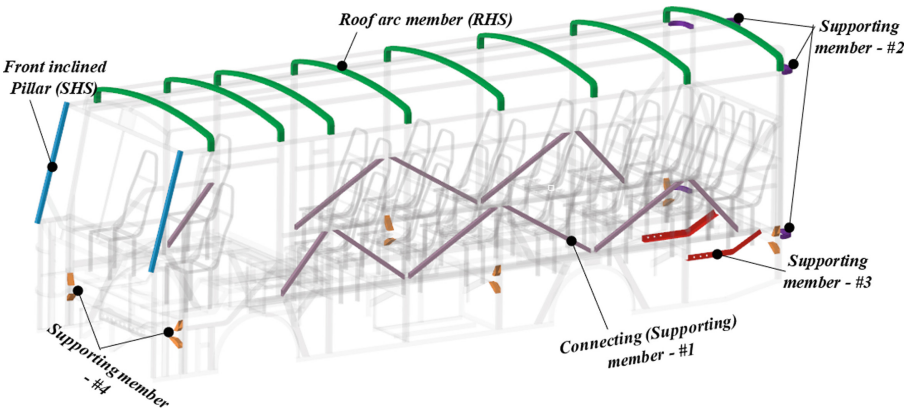

Fig. 9. Illustrates the improved configurations of the reinforced design

The comparison of masses of the components of baseline and reinforced configurations is described, as shown in Table 5. In sum, using this reinforcement design, the baseline model decreases its weight from 577.13 kg to 547.15 kg (29.98 kg).

Table 5. Components with its mass of baseline and reinforced (Model - I) configuration

Component		Cross-section		Quantity		Mass (kg)	
Baseline	Model - I	Baseline	Model - I	Baseline	Model - I	Baseline	Model - I
Front inclined pillar	Front inclined pillar	L-angle	SHS	2	2	2.26	4.53
Roof arc member	Roof arc member	SHS	RHS	8	8	36.06	44.74
Wall support member	Supporting member – #1	U – channel	SHS	44	11	77.11	19.7
–	Supporting member - #2	–	SHS	–	5	–	2.58
–	Supporting member - #3	–	L-Angle	–	2	–	7.86
–	Supporting member - #4	–	RHS	–	12	–	6.12
Total mass of the parts						115.43	85.53

Optimization Method via Successive Response Surface Method (SRSM)

Optimization methods using Response Surface Method (SRSM) are commonly used in design optimization of crashworthiness [34, 42, 73, 74]. Moreover, the main aim of this optimization is to maximize the reinforced structure's strength within a maintained level of weight during the rollover case. However, the analysis was carried out using LS – DYNA and LS-OPT (successive response surface method (SRSM)). Furthermore, the optimization task was done to identify the significance of the section of the reinforced structure in response to the loading experienced in ECE – R66 quasi-static testing procedures. From Eq. 6, the minimum requirement of absorbed energy of the reinforced design (Model – I) was equal to 4.86 kJ. Moreover, it is a fact that the highest value of energy absorption indicates a better strength of the structure. Consequently, Multi-objective optimization was done by reducing the total mass of the selected parts (objective function) and keeping the structure's energy absorption above 4.86 kJ (constraint). Thus, the energy absorption capacity should be greater than or equal to 4.86 kJ because the energy absorption capability is one of the parameters that indicates the structure's strength level. The energy absorption response was specified on the history output by integrating the structure's reaction force vs displacement. The interactive approach used to classify a

single best compromise solution by objective and constraint function [70]:

$$\begin{aligned} &\text{minimize} \quad f_1(t) \\ &\text{subject to} \quad f_2(t) \geq c \\ &\text{and } t \in \Omega \end{aligned} \tag{14}$$

where: Ω – sets of the lower and the upper bounds on inputs variable ($t_L \leq t \leq t_U$) and c – the bounds of the outputs ($c_{min} \leq c \leq c_{max}$).

And the only difference was that the constraint of this optimization is absorbed energy response. Furthermore, it can be expressed as:

$$\begin{aligned} &\text{Minimize the total mass of selected parts} \\ &\text{Subjected to: Absorbed Energy}(E_{st}) \geq 4.86 \text{ kJ} \end{aligned}$$

Figure 10 displays the selected parts of the structure for optimization tasks. In the design of experiments (DOE), The design variables are the thickness of the parts. First, these parts are grouped based on their assembly section. Then, the initial thickness values for these parts and the manufacturable lower and upper bounds (ranges) in the experiment design are listed, as shown in Table 6.

Table 6. The selected part's thickness and their range of values from reinforced structure

Sections	Symbols	Cross-section	Initial thickness (mm)	Ranges of mfg. values (mm)
Roof	troof	RHS & SHS	1.5	1, 1.5, 2, 2.5, 3
Rails	trail	SHS	1.5	1, 1.5, 2, 2.5, 3
Pillars	tplr	RHS	1.5	1, 1.5, 2, 2.5, 3

Figure 11 displays the optimization process to minimize the total mass of the structural member in the three thickness parameters (trail, troofa, and tplr) using LS-OPT. First, the three parameters are assigned for all selected parts in the Finite Element (FE) quasi-static model using LS – DYNA.

Moreover, it is imported to the optimization tool of LS-OPT. Then, linear ordered polynomial sampling is selected to identify the seven simulation points using D – optimal selection using LS-OPT. Next, the response of mass parts, internal energy, reaction force, and absorbed energy was formulated. Moreover, the output history of reaction force, displacement, and force vs. displacement plot were defined. Lastly, the objective and constraint of the optimization process was developed using a Genetic Algorithm for two iterations. The overall optimization iteration was performed within the linear response surface approximation. These approaches requested seven jobs per iteration. This means the optimization runs 14 + 1 jobs for all quasi-static simulations. Thus, the optimization approach using successive response surface methods took over ten days (238 h) for all simulations by Intel® Core™ i7-7700HQ CPU @ 2.80 GHz processor.

Study of Sensitivity via ANOVA and Global (GSA/Sobol)

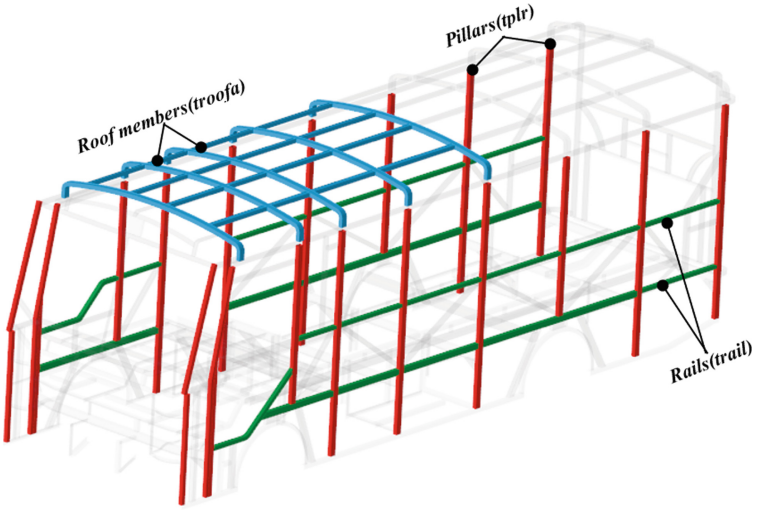

Fig. 10. Selected parts of the reinforced structure for quasi-static case optimization.

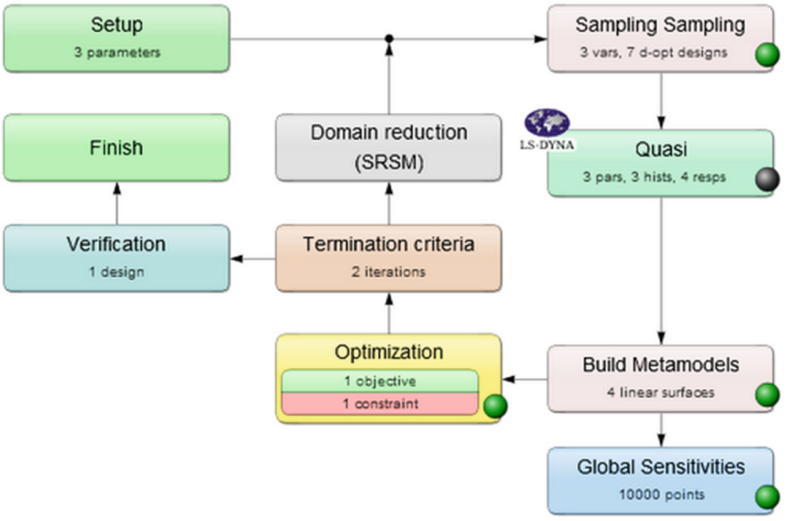

Fig. 11. Flow chart of the structural optimization of the reinforced structure in quasi-static simulation via LS-OPT

Figures 12 and 13 shows sensitivity analysis results for the total mass of the parts and responses absorbed energy by Global Sensitivity Analysis (GSA) with Sobol's and Analysis of Variance (ANOVA) approach. The trails and troofa are the minor influence variables for the mass parts. However, the thickness of the vertical pillars (tplr) is the

essential variable, and it has a 95% confidence interval of the response function. Moreover, the roof members also do not influence the response of absorbed energy, as shown in Fig. 13.

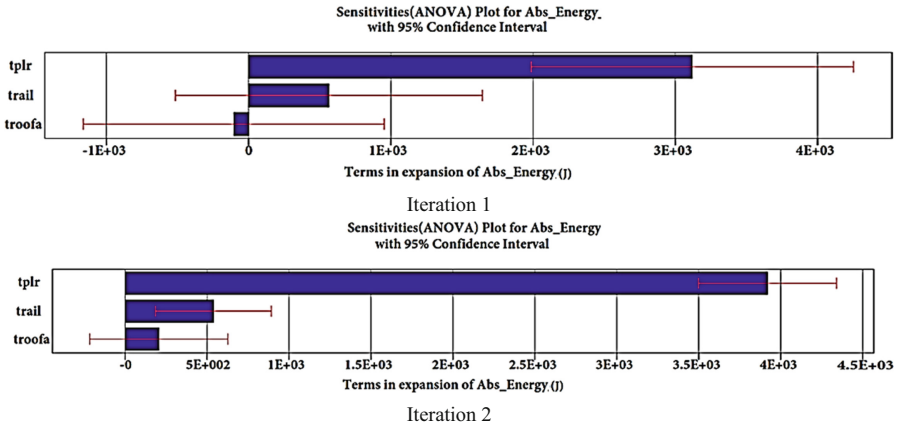

Fig. 12. Sensitivity (ANOVA) plot for the response of absorbed energy for all iterations

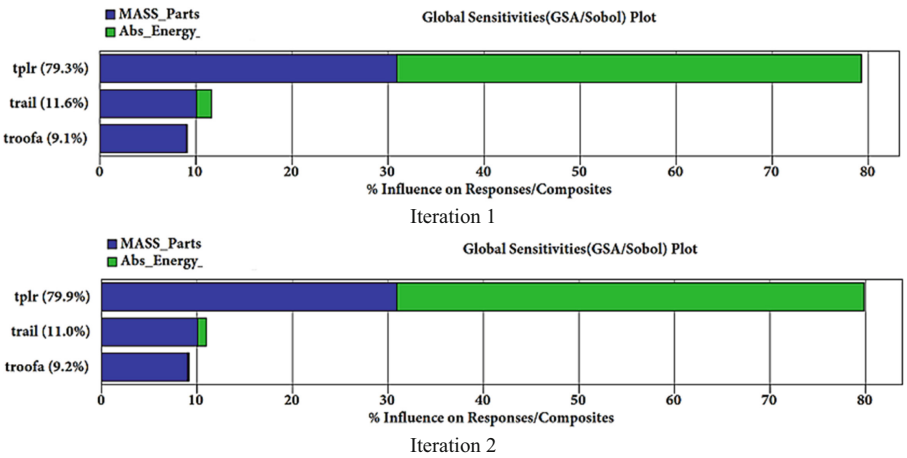

Fig. 13. Global Sensitivity (GSA/Sobol) plot for the response of mass of the parts and absorbed energy for all iterations

Figure 14 displays the tradeoff between the absorbed energy and total mass of the selected parts in all iterations. As shown in the first iteration of the design space, responses and design points have resulted in a most extensive and widely spread. Thus, the more focused design points are identified to obtain a new optimum result. During metamodel adequacy, when determining the best quality of the fit for responses, the error of root mean square (RMS) and the square (R^2) should be small and higher, respectively [46, 75]. Thus, the perfect fit ($R^2 = 1$) was found in both iterations for the mass parts response.

However, the R^2 of the absorbed energy response in the first and second iterations equals 0.987 and 0.999, respectively. This result denotes an almost perfect fit for all iteration.

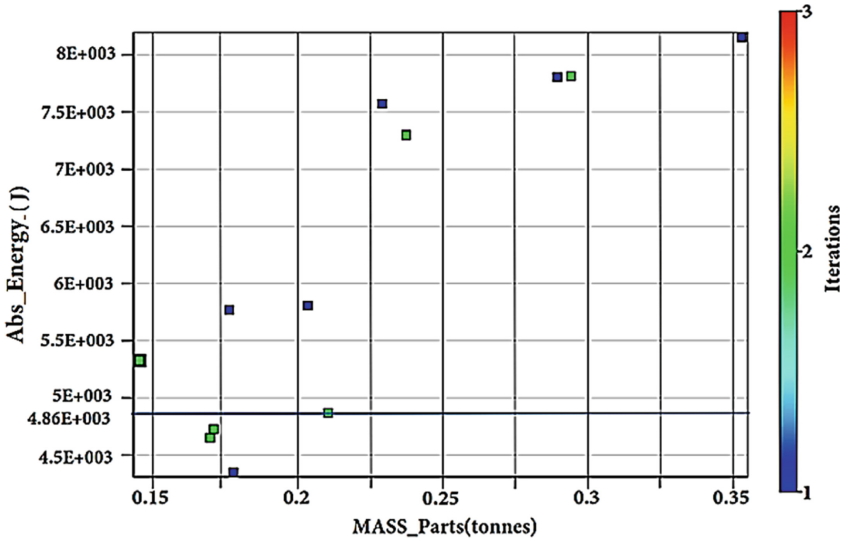

Fig. 14. The response of absorbed energy vs mass of the parts at the design variables

In Fig. 15, the optimization history presents the response of mass parts and absorbed energy. The decreasing rail and roof thickness reduced the mass of all parts from 0.176 tons (176 kg) to 0.145 tons (145 kg), equal to 17.6% (31 kg). At the same time, the increase of the thickness in the vertical pillars (*trail*) increases the value of absorbed energy. Moreover, it improves the energy absorbing capacity of the bus structure (energy requirement of ECE R66 Standard).

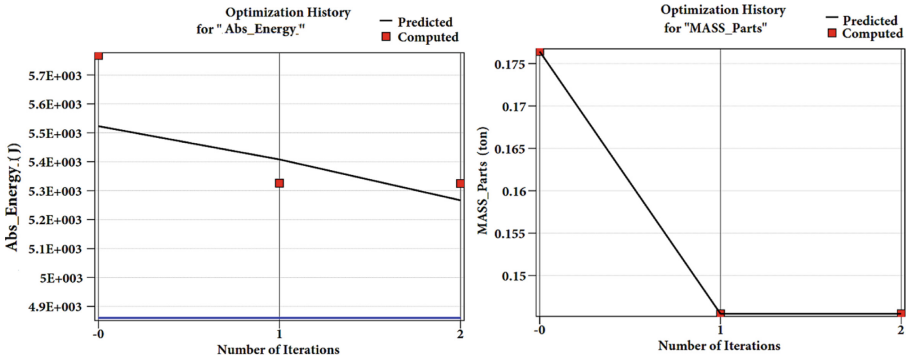

Fig. 15. Optimization history of the absorbed energy of the models (left) and the mass of the parts (right)

3 Result and Discussion

The reaction force and absorbed energy parameters were determined during a quasi-static simulation. The contour of stress specifies the maximum stress present at the contact area of impactor (rigid plate) loading, the joint areas of the vertical pillar-roof, and the vertical pillar-floor section, as shown in Fig. 16. A vertical pillar is highly intruded into residual space (RS) from the baseline simulation, as shown in Fig. 16 b). During the quasi-static simulation, the impactor load gradually increased until it touched the residual space. Perhaps, At the displacement of 375 mm, the simulation was motionless. Although the peak reaction forces for each model change differently based on the load resistance capacity. Figure 17(a) displays the reaction force developed on the baseline model, Model – I, and Model – II are 14.5 kN, 17.7 kN, and 16.3 kN. In addition, only the reinforced force converged after the displacement of 280 mm.

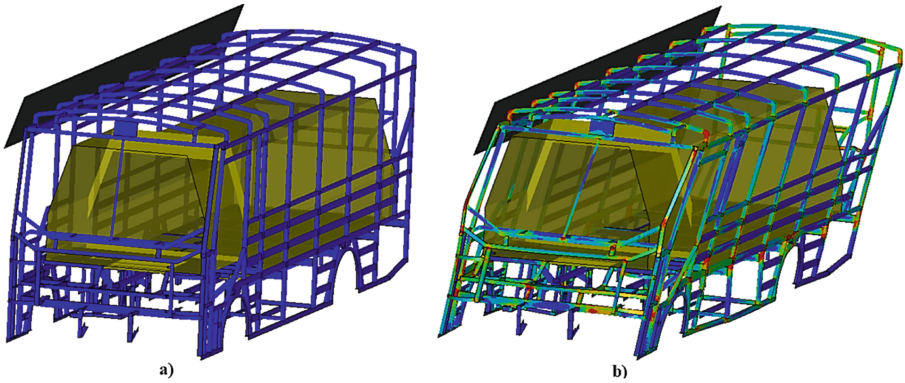

Fig. 16. Stress distribution in baseline model of quasi-static simulation: a) initial stage and b) final deformed condition

Figure 17(b) describes the minimum requirement of absorbed energies and energy absorbed by the structure (E_{st}) of the three structure models. The Absorbed energy of the baseline model, Model – I (RD), and Model – II (SRSM) are 4.43 kJ and 5.67 kJ, and 5.32 kJ, respectively. Accordingly, the energy-absorbing capability of the bus structure ($E_{st,ext}$) is lower than the minimum value of energy absorbed by the existing bus structure (E_{min}). This result also implies that the existing (existing) bus structure fails the tests cause one of the bays is touched the residual space. However, the reinforced energy absorption capacity ($E_{st,RD}$) is greater than the minimum requirement energy-absorbing structure ($E_{min,RD}$). Therefore, it was found that the reinforced structure passed the tests.

Moreover, model – II (SRSM) also passed the standard requirement. Notably, the reinforced Model (Model – I) is stronger than the baseline and Model – II (SRSM) models. This important finding is undoubtedly an equivalent method for the rollover test, as stated by UNECE R66.

Furthermore, all the models for the quasi-static analysis, shown in Fig. 18, follow the same deformation pattern when the cages' deformation is reached in a residual space.

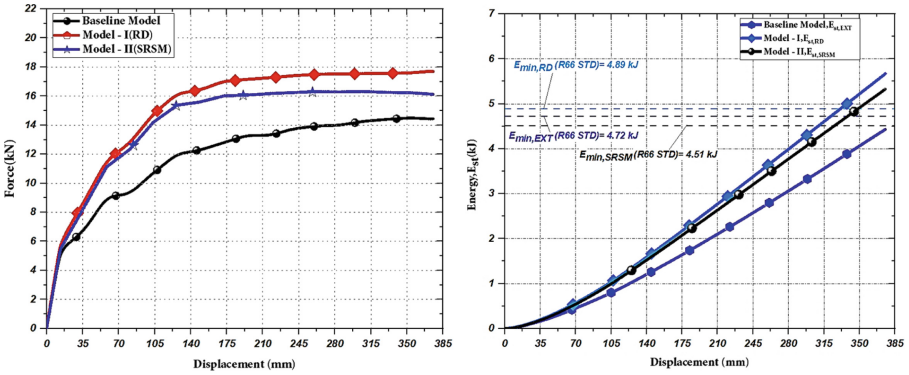

Fig. 17. Quasi-static simulation results for all models; a) Force versus displacement curves and b) Energy Absorption vs displacement curves

However, one of the baseline structural parts intruded the residual space, as shown in Fig. 18 a).

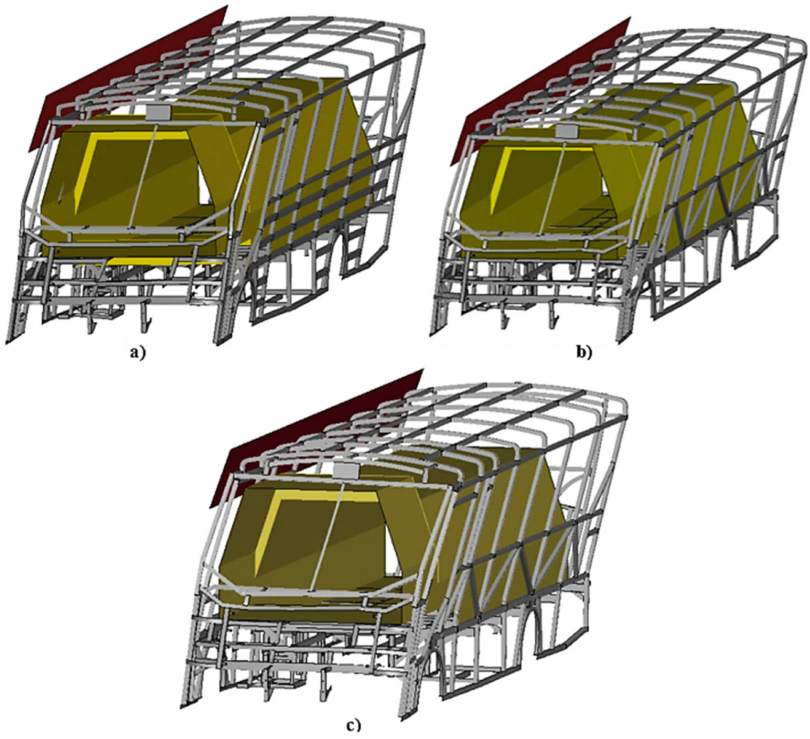

Fig. 18. Deformed models after quasi-static simulation: a) baseline model; b) model – I (RD); and c) model – II (SRSM)

The comparison of baseline and two alternative solutions using specific energy absorption capacity vs mass of the models were explained, as shown in Fig. 19. Thus, The Specific energy absorption of the Baseline model, Model – I, and Model – II are 7.68 J/kg, 10.36 J/kg, and 10.31 J/kg, respectively. This result shows that Model – I has a better energy absorption capacity than others. However, Model – II is more effective for better energy absorption capacity and less structure weight than others.

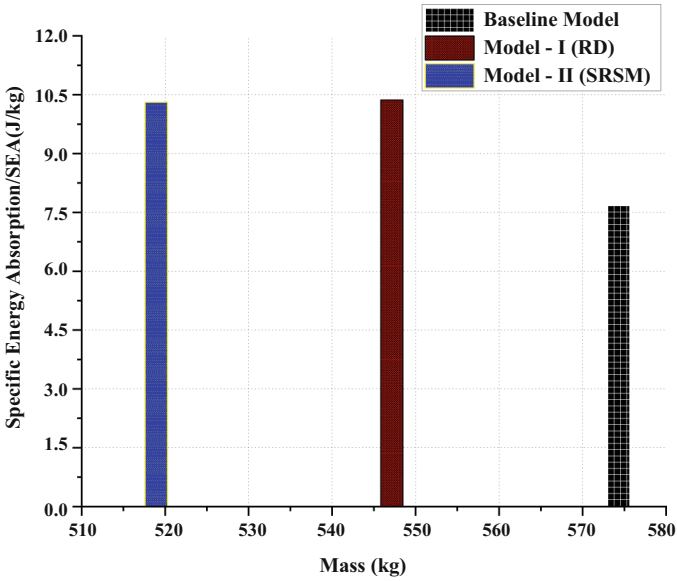

Fig. 19. Specific energy absorption vs mass of the three models

In a baseline (existing) tare–weight rollover case, the value of the internal energy of structure and seats are estimated. Significantly, the internal energy of the structure's main components and bus sections compared to visualize their capacity throughout the simulation. During the tare–weight rollover case, the maximum deformation of the existing structure and seat frame was located at pillar A and bays (B1 – B3), as shown in Fig. 20. Additionally, the high deformation of seats presents at the first and second seats of the passenger.

In the tare-weight rollover, the structure and seat's internal energies are 23.3 kJ and 0.85 kJ, respectively, as shown in Fig. 21. This result shows the internal energy of the structure is higher than the internal energy of the seat frames. Moreover, this finding shows that when the absorbed energy of the frame is higher, the structural part of the midibus is the most significant for the strength of the rollover case. A similar conclusion was reached by (Cezary Bojanowski, 2009), [46], where the author showed the effect of skin parts on the strength of a bus in a rollover crash test.

Although, the maximum internal energy for six sections of the structure is displayed, as shown in Fig. 22 (left). Accordingly, the minimum and maximum internal energy of 2.25 kJ and 6.56 kJ were obtained at the roof and right section of the bus structure because

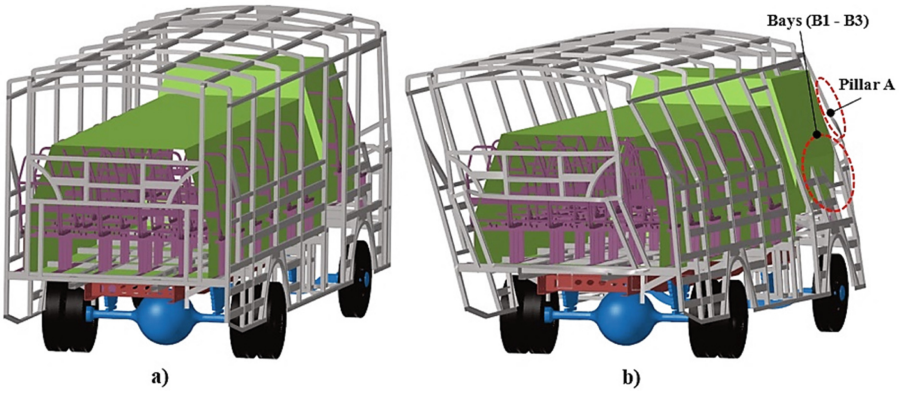

Fig. 20. Deformation of the existing structure and seats frame in tare – weight rollover case: a) initial phase and b) maximum deformation

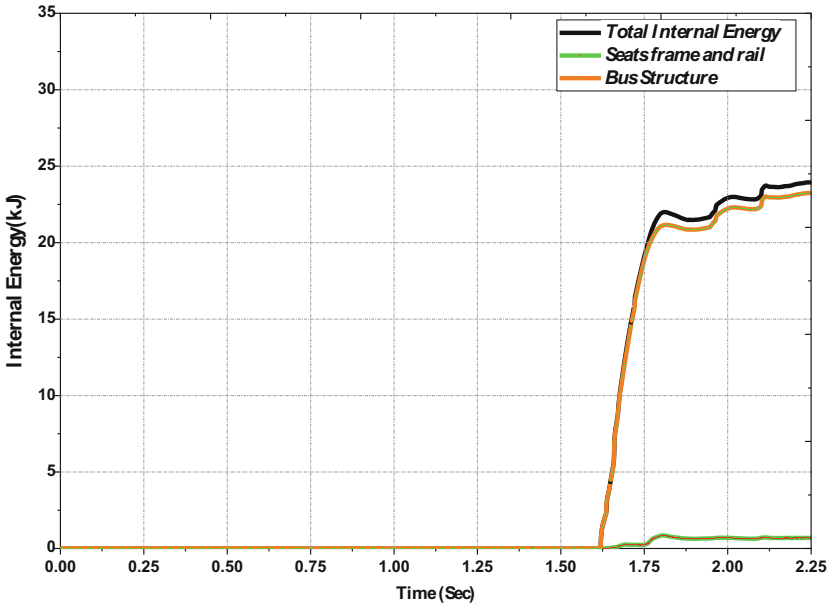

Fig. 21. Internal energy of the bus structure and seats in tare-loading cases

they are highly deformed until the rollover crash is stopped, leading to more energy absorption. Furthermore, the roof and front section have the lowest energy absorbing capacity because the rollover crash is not directly affected.

The sum of each component's internal energy contributes to the overall energy capability of the structure after the crash. In addition, Fig. 22 (right) shows the internal energy of each component. The absorbed energy of the components differs depending on the deformation throughout the crash. Hence, the internal energy of the A & B pillar, roof

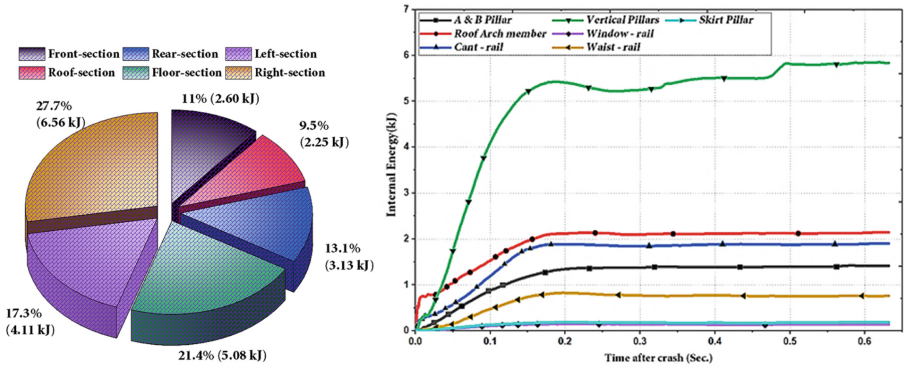

Fig. 22. Internal energy of the sections (left) and the components (right) of the baseline model in tare-weight rollover case

arc member, vertical pillars, window-rail, waist rail, and skirt pillar are 1.42 kJ, 2.15 kJ, 1.90 kJ, 5.85 kJ, 0.15 kJ, 0.83 kJ, and 0.19 kJ, respectively. This result shows that the lower and greater internal energy occurred at the window-rail and vertical pillar. Due to the high impact on the roof arc members and vertical pillar, the absorbed energy of these components is high compared to other components.

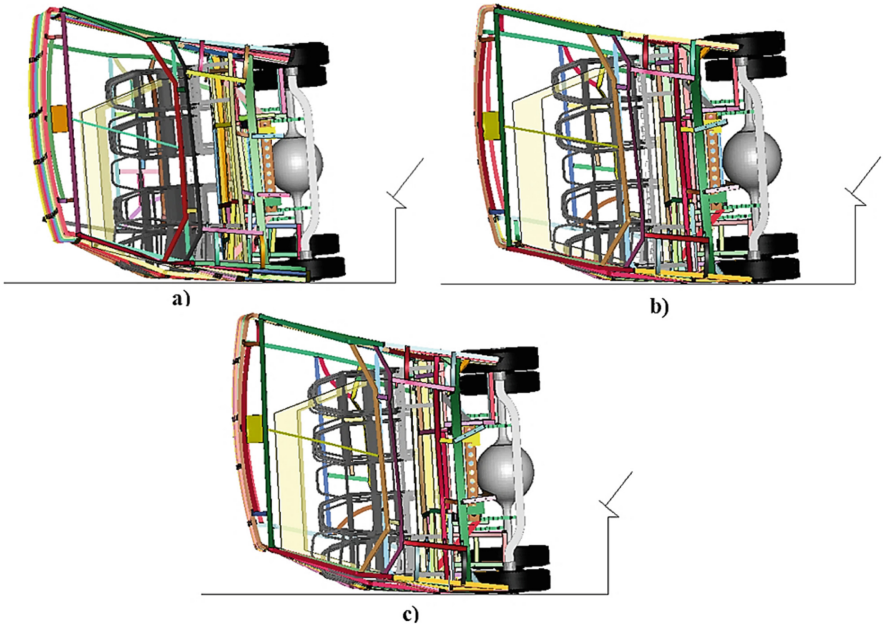

Fig. 23. Comparison of deformation in the tare-weight rollover: (a) Baseline model; (b) Model – I (RD); and (c) Model – II (SRSM)

In this section, angular deformation index and internal energy parameters are estimated to compare the crashworthiness capacity of the baseline model and alternative solutions during the tare-weight rollover scenario. The final deformations of these three models are displayed, as shown in Fig. 23. First, a baseline model is intruded on the residual space and is highly deformed (See Fig. 23 (a). Furthermore, model – II (SRSM) is less deformed than a baseline model. However, Model – I (RD) is less deformed than baseline and Model – II. Next, a model – I (RD) is less deformed than all models, and the residual space is far from the Model's frame, as shown in Fig. 23(b). Figure 24 displays the internal energy of the baseline model and two alternative designs in the tare – weight scenario. Thus, the internal energy of the baseline model, Model – I, and Model – II are 24.15 kJ, 28.3 kJ, and 25.7 kJ, respectively. As shown in Fig. 24, the internal energy of the baseline model, Model – I, and model – II are converged similarly from 0.0–0.2 s. The above results show that model – II (SRSM) has less weight with enough energy absorbing capacity than the baseline model.

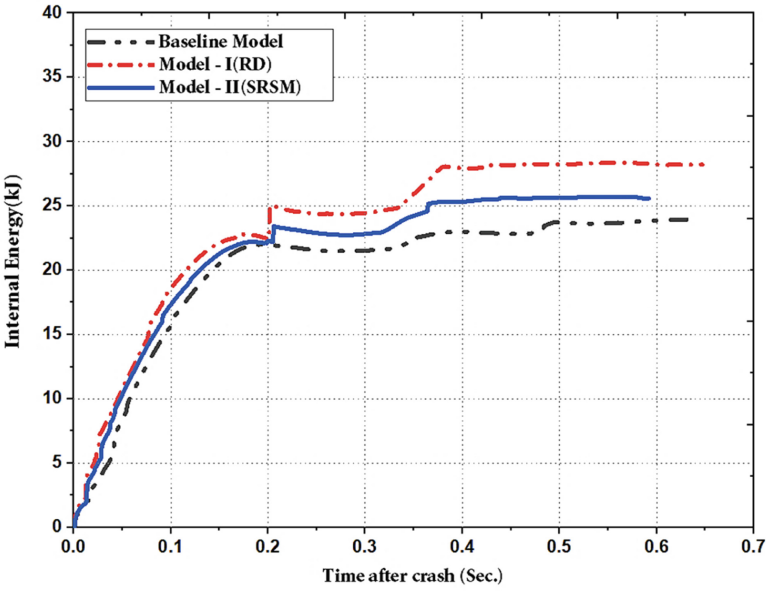

Fig. 24. Comparison of Internal energy between three models

The Angular deformation index (DI_θ) is another parameter to identify the crashworthiness capability of the structure during a rollover crash. Moreover, the angular deformation index of the structure response was measured based on angles between nodes with time in LS-DYNA. The rating of the angular deformation index (DI_θ) indicates the strength of structure during structural deformation. Therefore, this section evaluates the angular deformation index to compare the three models in tare-weight rollover simulation. The maximum DI_θ of the baseline model, Model – I and Model – II are 1.07, 0.70, and 0.78, respectively, as shown in Table 7. These maximum deformation indexes are located at pillar A with bays (B1–B3) for all models in the tare-wight rollover scenario

except Model – III (bays (B4–B8)). As depicted in Table 7, the change of plastic hinge angles and the maximum angular deformation index at the pillar and bays of the structure are described in the tare-weight scenarios for all three models.

Table 7. Comparison of deformation index among three models in tare-weight scenario

Change of angles (deg) and DI	Pillar A & bays (B1–B3)			Bays (B4–B8)		
	Baseline	M- I (RD)	M-II (SRSM)	Baseline	M- I (RD)	M-II (SRSM)
$\Delta\theta_1$	−32.9	−19.6	−22.7	5.8	2.2	2.6
$\Delta\theta_2$	2.6	8.4	12.0	0.6	0.5	0.5
$\Delta\theta_3$	17.5	7.6	6.8	−17.8	−8.4	−10.7
$\Delta\theta_4$	26.4	18.2	21.9	18.8	−12.3	−20.4
$\Delta\theta_5$	6.5	9.4	13.1	21.4	11.9	21.5
$\Delta\theta_6$	−10.9	−3.9	−2.8	5.9	3.2	3.1
DI_θ	1.07	0.70	0.78	0.69	0.40	0.59

Figure 25 compares the deformation index vs time curves of the baseline model and alternative models in the tare – weight rollover case. In this scenario, the baseline structure has an unacceptable and poor strength. This strength describes that the entire structure failed due to high deformation at pillar A and bays (B1-B3). These results imply that the total structural strength of the baseline model is weak to survive in this rollover crash case. Moreover, both Model – I (RD) and Model – II (SRSM) have acceptable strength in tare–weight cases.

4 Conclusion

This research paper also facilitates the rollover crashworthiness capability of the structure in quasi-static loading and tare-weight rollover scenarios. In addition, the two alternative designs for rollover were conducted using reinforcement design and optimization by successive response surface method using LS-OPT for all quasi-static and rollover analyses. From both analysis and optimization results, the following conclusions are mentioned:

- The energy absorption of the existing (baseline) model is less than the minimum requirement energy by ECE R66 in quasi-static simulation, which means the existing bus structure fails the rollover tests due to one of the bays is touched the residual space. However, all design alternative solutions pass the test because of fulfilling the requirement of the standard.
- During the tare-weight rollover case, the baseline structure and seat frame contain 96.5% and 3.5% of internal energy, respectively. The entire structure failed due to

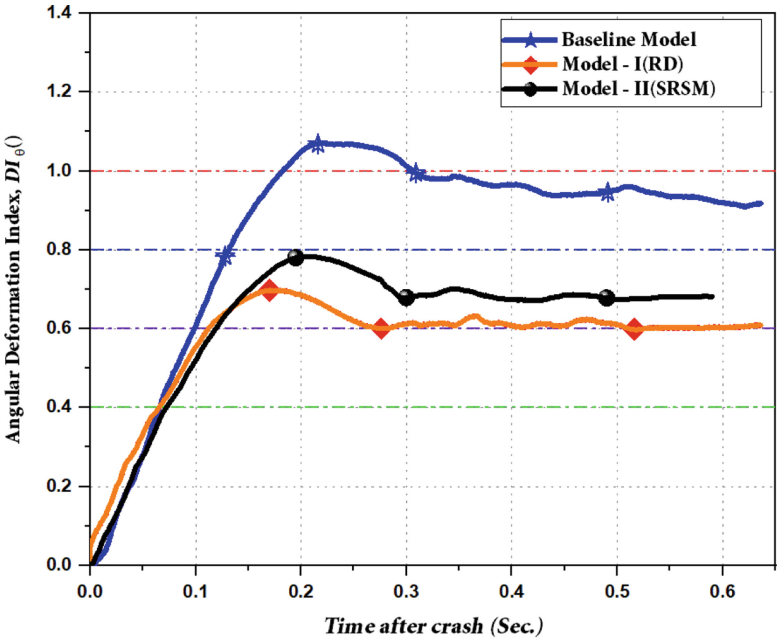

Fig. 25. Comparison of deformation index between three models

high deformation at pillar A and bays (B1–B3). Moreover, the lower and greater internal energy occurred at the skirt and vertical pillars. As per the tare – weight rollover analysis and optimization results of baseline and two alternative models, the internal energy and angular deformation index (DI_θ) are the main parameters to identify the crashworthiness capacity.

Generally, it can be determined that the baseline model, Model – I (RD), and Model – II (SRSM) have unacceptable, acceptable, and intermediate strengths, respectively. Therefore, the first design approach is that the reinforced design experiences sufficient strength by adding the support and change of cross-section on the front pillars. Moreover, a model – II (SRSM) has less weight with adequate energy absorbing capacity than a reinforced model by varying the thickness of pillars, windows, and waist rails. Moreover, a model – II (SRSM) has less weight with adequate energy absorbing capacity than a baseline model.

References

1. Addisu, H.S., Koricho, E.G.: Structural weight and stiffness optimization of a midibus using the reinforcement and response surface optimization (RSO) method in static condition. Model. Simul. Eng. **2022**, 1–15 (2022)
2. Bai, J., Meng, G., Zuo, W.: Rollover crashworthiness analysis and optimization of bus frame for conceptual design. J. Mech. Sci. Technol. **33**(7), 3363–3373 (2019)

3. Bin Yusof, M., Amirul, M., Bin, A.: Effect of mass on bus superstructure strength having rollover crash. Int. Sci. Index **6**(8), 1443–1449 (2012)
4. Karliński, J., Ptak, M., Działak, P., Rusiński, E.: Strength analysis of bus superstructure according to Regulation No. 66 of UN/ECE. Arch. Civil Mech. Eng. **14**(3), 342–353 (2013)
5. Tulu, G.S., Washington, S., King, M.J.: Characteristics of police-reported road traffic crashes in ethiopia over a six year period. In: Proceedings of the 2013 Australasian Road Safety Research, pp. 1–13 (2013)
6. UNECE 2004: Statistics about rollover accident of buses – VI. Hungary (2004)
7. UNECE 2020: Road Safety Performance Review – Ethiopia. United Nations Economic Commission for Africa & Europe, Geneva **20** (2020)
8. Tech, T.W., Iturrioz, I., De Meira Júnior, A.D.: Numerical simulation of bus rollover. SAE Tech. Pap. (2007)
9. Iozsa, M. D., Micu, D. A. N. A., Frățilă, G.: Influence of crash box on automotive crashworthiness. Recent Adv. Civ. Eng. Mech. 49–54 (2014)
10. Series, N.A.S.I., Base, N.: Crashworthiness of Transportation Systems: Structural Impact and Occupant Protection (1997)
11. Cezary, B. Jerry, W., Leslaw, K., Jerzy, K.: Florida standard for crashworthiness and safety evaluation of paratransit buses. Transit Off. Florida Dep. Transp. 1–14 (2009)
12. Micu, D.A., Iozsa, D., Stan, C.: Quasi-static simulation approaches on rollover impact of a bus structure. In: WSEAS, ACMOS, pp. 81–86 (2014)
13. Nurhadi, I., Zain, R.: Development of computer based procedure for quantitative evaluation of bus superstructure in type approval. J. KONES **17**(2), 371–378 (2010)
14. Mohd Nor, M.K., Dol Baharin, M.Z.: Rollover analysis of heavy vehicle bus. Appl. Mech. Mater. **660**, 633–636 (2014)
15. Na, J., Wang, T., Xu, Z.: Research on a one-step fast simulation algorithm for bus rollover collision based on total strain theory. Int. J. Crashworthiness **19**(3), 275–287 (2014)
16. Mahajan, R.S., Daphal, P.N., Athavale, S.M.: Study and analysis of rollover resistance of bus body structure by non-linear FEM technique and experimental method. In: SAE Tech. Pap., pp. 205–209 (2003)
17. Zhou, W., Kuznectov, A., Wu, C.Q., Telichev, I.: A comparative numerical study of motor-coach rollover resistance under ECE R66 and proposed NHTSA regulation conditions. Int. J. Crashworthiness **25**(2), 1–16 (2019)
18. Phadatare, V.D.: Performance improvement of bus structure for rollover analysis using FEA and validation of roll bar. IOSR J. Mech. Civ. Eng. **17**(10), 16–19 (2017)
19. Thosare, A., Patil, S.B.: Rollover analysis of bus body to meet ais-052 regulations and optimization of the body. Int. Eng. Res. J. **3**, 96-102 (2017)
20. Rogov, P.S., Orlov, L.N.: Verification of computer simulation results of bus body section rollover. J. Traffic Transp. Eng. **3**(2), 118–127 (2015)
21. Yang, L., Deng, S.: Structural local analysis and optimization of bus body skeleton. In: 5th International Conference Civil Engineering Transportation no. ICCET, pp. 1975–1979 (2015)
22. Korta, J., Uhl, T.: Multi-material design optimization of a bus body structure. J. KONES. Powertrain Transp. **20**(1), 139–146 (2013)
23. Reyes-ruiz, C., Cervantes, O.R., Prado, A.O., Ramirez, E.: Analysis and optimization of a passenger bus frame through finite element software. In: 2013 SIMULIA Community Conference (2013)
24. Bin Yusof, M., Bin Afripin, M.A.A.: Effect of beam profile size on bus superstructure strength having rollover crash. Appl. Mech. Mater. **372**, 620–629 (2013)
25. Hu, H., Yang, C.L., Wang, J.: Development and validation of finite element model for the welded structure of transit bus. Int. J. Heavy Veh. Syst. **19**(4), 371–388 (2012)
26. Li, Y., Lan, F., Chen, J.: Experimental and numerical study of rollover crashworthiness of a coach body section. SAE Int., vol. 8 (2012)

27. Su, R., Gui, L., Fan, Z.: Multi-objective optimization for bus body with strength and rollover safety constraints based on surrogate models. Struct. Multidiscip. Optim. **44**(3), 431–441 (2011)
28. Bojanowski, C., Kulak, R.F.: Multi-objective optimisation and sensitivity analysis of a para-transit bus structure for rollover and side impact tests. Int. J. Crashworthiness **16**(6), 665–673 (2011)
29. Tech, T.W., Iturrioz, I.: Structural optimization of a bus in rollover conditions. SAE Tech. Pap. (2009)
30. Matolcsy, M.: The severity of bus rollover accidents. Crashworthiness Transp. Syst. 07 (1997)
31. Friedman, K., Hutchinson, J., Weerth, E., Mihora, D.: Implementation of composite roof structures in transit buses to increase rollover roof strength and reduce the likelihood of rollover. Int. J. Crashworthiness **11**(6), 593–596 (2006)
32. Lin, Y.C., Nian, H.C.: Structural design optimization of the body section using the finite element method. SAE Tech. Pap. (2006)
33. Lan, F., Chen, J., Lin, J.: Comparative analysis for bus side structures and lightweight optimization. Proc. Inst. Mech. Eng. Part D J. Automob. Eng. **218**(10), 1067–1075 (2004)
34. Liang, C.C., Le, G.N.: Bus rollover crashworthiness under European standard: An optimal analysis of superstructure strength using successive response surface method. Int. J. Crashworthiness **14**(6), 623–639 (2009)
35. Rahman, M.K.: Body section analysis in bus rollover simulation. J. East. Asia Soc. Transp. Stud. **9**, 1967–1981 (2011)
36. Park, S.J., Yoo, W.S., Kwon, Y.J.: Rollover analysis of a bus using beam and nonlinear spring elements. WSEAS Trans. Math. **5**(5), 526–531 (2006)
37. Liang, C.C., Nam, L.G.: Comparative analysis of bus rollover protection under existing standards. WIT Trans. Built Environ. **113**, 41–53 (2010)
38. Subic, A., He, J.: Improving bus rollover design through modal analysis. Int. J. Crashworthiness **2**(2), 139–152 (1997)
39. Bojanowski, C., Gepner, B., Kwasniewski, L., Rawl, C., Wekezer, J.: Roof Crush Resistance and Rollover Strength of a Paratransit Bus. In: 8th European LS-DYNA® Users Conference, vol. 66, no. May 2011, pp. 1–13 (2011)
40. Valladares, D., Miralbes, R., Castejon, L.: Development of a numerical technique for bus rollover test simulation by the F.E.M. In: WCE 2010 - World Congress on Engineering 2010, vol. 2, pp. 1361–1365 (2010)
41. Liu, Y.: ANSYS and LS-DYNA used for structural analysis. Int. J. Comput. Aided Eng. Technol. **1**(1), 31–44 (2008)
42. Gepner, B.D.: Rollover Procedures for Crashworthiness Assessment of Paratransit Bus Structures. Florida State University (2014)
43. UNECE R66: Uniform technical prescriptions concerning the approval of large passenger vehicles with regard to the strength of their superstructure. Geneva (2006)
44. Schweizerhof, K., Walz, M., Rust, W.J.H., Franz, U.: Quasi-static analyses using explicit time integration - applications of LS-DYNA. In: 2nd Eur. LS-DYNA Conference, no. May 2018, pp. 1–18 (1999)
45. Gertsch, J., Shim, T.: Interpretation of roll plane stability models. Int. J. Veh. Des. **46**(1), 72–93 (2008)
46. Bojanowski, C.: Verification , Validation and Optimization of Finite Element Model of Bus Structure for Rollover Test. Florida State University (2009)
47. Kwa, L., Wekezer, J.W., Gepner, B., Siervogel, J.: Development of simplified safety assessment procedure for paratransit buses. Comput. Methods Mech., no. 028818 (2011)
48. Wekezer, J.W., Cichocki, K.: Structural response of paratransit buses in rollover accidents. Int. J. Crashworthiness **12**(3), 217–225 (2007)

49. Guler, M.A., Elitok, K., Bayram, B., Stelzmann, U.: The influence of seat structure and passenger weight on the rollover crashworthiness of an intercity coach. Int. J. Crashworthiness **12**(6), 567–580 (2007)
50. Boria, S.: Lightweight Design and Crash Analysis of Composites. Elsevier Ltd. (2016)
51. Wicaksono, S., Rizka Faisal Rahman, M., Mihradi, S., Nurhadi, I.: Finite element analysis of bus rollover test in accordance with UN ECE R66 standard. J. Eng. Technol. Sci. **49**(6), 799–810 (2017)
52. Isuzu Motors Limited. Isuzu N-Series Body Builders Guide (2014)
53. General Motors Isuzu Commercial Truck and American Isuzu motors Inc. Isuzu Body Builder's Guide (2003)
54. Isuzu Motors Inc.: Isuzu N-Series Body Builder Guides. www.isuzutruckservice.com%0ADownload (2016)
55. Bitzenbauer, J., Franz, U., Schweizerhof, K.: Deformable Rigid Bodies in LS-DYNA with Applications – Merits and Limits (2005)
56. LSTC 2021: Hourglass-Welcome to the LS-DYNA support site. Livermore Software Technology Corporation (LSTC). https://www.dynasupport.com/howtos/element/hourglass. Accessed 19 May 2021
57. Seyedi, M., Jung, S., Wekezer, J.: A comprehensive assessment of bus rollover crashes : integration of multibody dynamic and finite element simulation methods. Int. J. Crashworthiness **27**(3), 1–16 (2020)
58. Wang, Q., Zhou, W., Telichev, I., Wu, C.Q.: Load transfer analysis of a bus bay section under standard rollover test using U*M index. Int. J. Automot. Technol. **19**(4), 705–716 (2018)
59. Elseufy, S.M., Mawsouf, N.M., Ahmad, A.: Safety evaluation of buses during rollover. J. Manag. Eng. Integr. **6**(March), 102–108 (2013)
60. Chirwa, E.C., Li, H., Qian, P.: Modelling a 32-seat bus and virtual testing for R66 compliance. Int. J. Crashworthiness **20**(2), 200–209 (2015)
61. Kwasniewski, L., Bojanowski, C., Siervogel, J., Wekezer, J.W., Cichocki, K.: Crash and safety assessment program for paratransit buses. Int. J. Impact Eng. **36**(2), 235–242 (2009)
62. Livermore Software Technology Corporation, Keyword User's Manual Vol II, vol. I, no. May (2007)
63. Rabbat, B.G., Russell, H.G.: Friction coefficient of steel on concrete or grout. J. Struct. Eng. **111**(3), 505–515 (1985)
64. Gleba, M.: Effect of Friction on Vehicle Crashworthiness during Rollover. Florida State University Libraries (2015)
65. Zhu, L.: Development of guidelines for deformable and rigid switch in Ls-Dyna simulation. University of Nebraska (2009)
66. Zhou, W., Kuznetcov, A., Telichev, I., Wu, C.: Deformable-rigid switch in computational simulation of bus rollover test. Int. Union Theor. Appl. Mech., no. August, pp. 3–4 (2016)
67. Hamid, I.A., Kamarudin, K.A., Osman, M.R., Abidin, A.N.S.Z., Zulkipli, Z.H.: Finite element bus rollover test verification. J. Soc. Automot. Eng. Malaysia **3**(4), 57–63 (2019)
68. LSTC 2021: Total energy-Welcome to the LS-DYNA support site. Livermore Software Technology Corporation (LSTC). https://www.dynasupport.com/howtos/general/total-energy. Accessed 19 May 2021
69. LSTC 2021: Energy data-Welcome to the LS-DYNA support site. Livermore Software Technology Corporation (LSTC). https://www.dynasupport.com/tutorial/ls-dyna-users-guide/energy-data. Accessed 19 May 2021
70. Belegundu, A.D., Chandrupatla, T.R.: Optimization Concepts and Applications in Engineering, 3rd ed. Cambridge University Press (2019)
71. Vanderplaats, G.N.: Structural optimization for statics, dynamics and beyond. J. Brazilian Soc. Mech. Sci. Eng. **28**(3), 316–322 (2006)

72. Witteman, W.J.: Improved Vehicle Crashworthiness Design by Control of the Energy Absorption for Different Collision Situations, Thesis, 1999, Eindhoven University of Technology, ISBN 90-386-0880-2, no. 1999 (1999)
73. Kurtaran, H., Eskandarian, A., Marzougui, D., Bedewi, N.E.: Crashworthiness design optimization using successive response surface approximations. Comput. Mech. **29**(4–5), 409–421 (2002)
74. Esfahlani, S.S., Shirvani, H., Nwaubani, S., Shirvani, A., Mebrahtu, H.: Comparative study of honeycomb optimization using Kriging and radial basis function. Theor. Appl. Mech. Lett. **3**(3), 031002 (2013)
75. Stander, N., Roux, W., Goel, T., Eggleston, T., Craig, K.: LS – OPT User's Manual: A Design Optimization and Probabilistic Analysis Tool. Livermore Softw. Technol. Corp., no. February (2012)